PROCEEDINGS OF SPIE

SPIEDigitalLibrary.org/conference-proceedings-of-spie

Numerical simulation of the spectrum of secondary acoustic-gravity waves in the middle and upper atmosphere

Matvey Efimov, Nikolai Gavrilov, Sergey Kshevetskii, Andrey Koval

Matvey M. Efimov, Nikolai M. Gavrilov, Sergey P. Kshevetskii, Andrey V. Koval, "Numerical simulation of the spectrum of secondary acoustic-gravity waves in the middle and upper atmosphere," Proc. SPIE 12780, 29th International Symposium on Atmospheric and Ocean Optics: Atmospheric Physics, 127807C (17 October 2023); doi: 10.1117/12.2690531

Event: XXIX International Symposium "Atmospheric and Ocean Optics, Atmospheric Physics", 2023, Moscow, Russian Federation

Numerical Simulation of the Spectrum of Secondary Acoustic-Gravity Waves in the Middle and Upper Atmosphere

Matvey M. Efimov*[a], Nikolai M. Gavrilov[a], Sergey P. Kshevetskii[b], Andrey V. Koval[a]

[a]Atmospheric Physics Department, Saint-Petersburg State University, 7/9 Universitetskaya emb., Saint Petersburg, 199034, Russia. [b]Institute of Physical and Mathematical Sciences and Information Technology, Immanuil Kant Baltic Federal University, 14 Alexander Nevsky Street, Kaliningrad, 236041, Russia.

ABSTRACT

Increased attention is currently paid to studying the so-called "secondary" acoustic-gravity waves (AGWs), which appear due to instabilities and nonlinear interactions of "primary" wave modes generated by atmospheric sources. This report is devoted to the study of horizontal spatial spectra of primary and secondary AGWs at fixed altitude levels in the middle and upper atmosphere using a high-resolution three-dimensional nonlinear model AtmoSym. It is found that in a short time after turning on the source of plane waves at the lower boundary of the model, the spectrum contains mainly a peak related to the primary AGW. Later, spectral peaks corresponding to secondary AGWs appear at horizontal wave numbers that are multiples of the wave numbers of the primary wave. This study allows estimating relative contributions of secondary AGWs at different heights, different times, and for different atmospheric conditions.

Keywords: acoustic-gravity waves, spectrum, secondary waves, numerical simulation, upper atmosphere, middle atmosphere.

1. INTRODUCTION.

Important factors of the middle and upper atmosphere dynamics are acoustic-gravity waves (AGWs). They are generated in the lower atmosphere and propagate upwards, transmitting energy and momentum to the middle and upper atmosphere. Dissipating waves can influence zonal and meridional circulation in the mesosphere and lower thermosphere (MLT) region. Recent studies demonstrate the AGW importance for the thermosphere [1, 2]. These studies revealed that accelerations of the mean flow created by dissipating AGWs contribute to maintaining the momentum balance in the thermosphere. Thus, proper knowledge about AGWs is necessary for understanding the dynamics of the middle and upper atmosphere. Recently, numerical simulations of nonlinear AGWs and turbulence in the atmosphere has been intensively expanding. Fritts et al. [3, 4] simulated the breaking of atmospheric waves and developing Kelvin-Helmholtz instabilities. These three-dimensional models simulate AGW propagation and breaking in atmospheric areas having restricted vertical and horizontal sizes. Authors [5, 6] made two-dimensional simulations of atmospheric AGWs.

When AGWs are destroyed in the middle and upper atmosphere, they produce strong nonlinearity and cascade energy transfer to smaller scale “secondary” wave modes having lengths smaller than the primary AGWs. These secondary AGWs can activate the transition of wave energy to turbulence, and can also create significant wave momentum fluxes. In addition, secondary AGWs can form background field inhomogeneities with dimensions comparable to the horizontal dimensions of wave packets [8]. Primary AGWs that propagate from the troposphere can create localized areas of increased and decreased momentum and energy fluxes in the middle and upper atmosphere [9, 10]. Secondary AGWs can also be generated by strong nonlinearities during the destruction of primary AGWs. Such secondary AGWs appear as "high harmonics" and usually have lengths and periods shorter than primary wave modes [11, 12]. Thus, the generation of secondary AGWs is an important and little studied process that strongly modifies the mechanisms of transfer and transformation of wave energy and momentum. A deeper study of secondary AGWs requires the development of high-resolution numerical models and methods of proper spectral analysis.

A high-resolution three-dimensional numerical model of nonlinear AGW propagation from the Earth's surface to the thermosphere has been developed by Gavrilov and Kshevetskii [7]. The numerical scheme involves the fundamental conservation laws for energy, mass and momentum, also the non-decreasing entropy law.

*matvey.efimov.96@mail.ru; phone 8-962-701-08-40

29th International Symposium on Atmospheric and Ocean Optics: Atmospheric Physics,
edited by Oleg A. Romanovskii, Proc. of SPIE Vol. 12780, 127807C

This model allows obtaining physically correct solutions of hydrodynamic equations, and ensure the numerical scheme stability in the region of breaking of nonlinear AGWs into turbulence, where many computational algorithms become ineffective. In combination with a large range of studied heights, this stable algorithm makes this numerical model suitable for modeling AGWs and their instabilities at heights from the earth's surface to the thermosphere. Numerical modeling makes it possible better understanding the mechanisms of dynamic interaction between different layers of the atmosphere.

A high-resolution three-dimensional numerical model of nonlinear AGW propagation from the Earth's surface to the thermosphere has been developed by Gavrilov and Kshevetskii [7]. The numerical scheme involves the fundamental conservation laws for energy, mass and momentum, also the non-decreasing entropy law. This model allows obtaining physically correct solutions of hydrodynamic equations, and ensure the numerical scheme stability in the region of breaking of nonlinear AGWs into turbulence, where many computational algorithms become ineffective. In combination with a large range of studied heights, this stable algorithm makes this numerical model suitable for modeling AGWs and their instabilities at heights from the earth's surface to the thermosphere. Numerical modeling makes it possible better understanding the mechanisms of dynamic interaction between different layers of the atmosphere.

This paper describes simulating plane waves in the high-resolution AtmoSym model involving an algorithm that allows separating a spectrum of primary AGWs generated by a wave source at the lower boundary of the model from the spectrum of secondary AGWs that are generated at different levels of the middle and upper atmosphere by these primary waves. Examples are given showing the gradual formation of the spectrum of secondary waves after sharp triggering on the wave source in the model.

2. NUMERICAL MODEL.

In this study, we use a high-resolution 3D numerical model, called as “AtmoSym”, for nonlinear atmospheric AGWs [7], which is now available for free online use [13]. This model uses flat geometry and primitive 3D hydrodynamic equations [7]. The AtmoSym model involves dissipative and nonlinear processes affecting the propagation of AGWs. The background coefficients of dynamic molecular viscosity and thermal conductivity are estimated using the Sutherland formula [14]. The AtmoSym model includes also background turbulent viscosity and thermal conductivity, reaching maxima of about 10 m^2/s in the boundary layer and lower thermosphere and a minimum of 0.1 m^2/s in the stratosphere [7]. Zero values of vertical temperature and horizontal velocity gradients, as well as zero vertical velocity are set on the upper boundary [7]. Such upper boundary conditions can cause the reflection of AGWs coming from the underlying layers of the atmosphere. The upper boundary in the present study is set at altitude of 600 km, where the molecular viscosity and thermal conductivity are very high and the reflected waves are subject to strong attenuation. Numerical tests show that the influence of the upper boundary conditions is negligible at distances from the upper boundary that exceed twice the height scale of the atmosphere. Therefore, at altitudes up to 200 km, analyzed in this article, the influence of the upper boundary conditions is insignificant. The lower boundary conditions on the Earth's surface have the following form (see [7]):

$$(T')_{z=0} = 0, \quad (u)_{z=0} = 0, \quad (v)_{z=0} = 0, \quad (w)_{z=0} = W_0 \, cos(\sigma t - \overrightarrow{k_h} \cdot \vec{r}), \tag{1}$$

where T', u, v, $w$are wave perturbations of temperature and velocity components along the horizontal axes x, y and the vertical axis z, respectively. The last relation for the vertical velocity on the Earth's surface in (1) serves as a source of flat AGWs in the AtmoSym model, with W_0 and σ being the amplitude and frequency of wave excitation; $\overrightarrow{k_h}(k_x, k_y)$ and $\overrightarrow{r_h}(x, y)$ are the horizontal wave vector and radius vector, and k_x and k_y are the wave numbers along the horizontal axes x and y, respectively. Plane wave modes can be considered as spectral components of tropospheric convective, turbulent and meteorological processes. These processes can be parameterized by the corresponding sets of effective spectral components of the vertical velocity at the lower boundary of the atmosphere [15, 16]. Along the horizontal axes x and y, one can assume the periodicity of the wave fields.

Our numerical simulation starts from a steady and windless state of the undisturbed atmosphere with vertical background temperature, density, molecular weight, and molecular-kinematic viscosity profiles corresponding to January at a latitude of 50° N at the mean solar activity according to the NRLMSISE-00 model [17]. The wave source in the model is sharply activated at $t = 0$, and for $t > 0$ the source amplitude W_0 in (1) does not change. It should be expected that at small amplitudes of the wave source in equation (1), in the lower and middle atmosphere at $t » 0$, the numerical solution should tend the steady plane AGWs corresponding to the standard linear theory (for example, [18]). Gavrilov et al. [19] showed good agreement between the simulated amplitudes of various wave fields and the polarization relations of the linear AGW theory [18] at $t \gg 0$ at altitudes up to 100 km.

3. RESULTS OF SIMULATIONS

In the present study, we consider AGW modes propagating along the eastward x axis and assume, similarly to [20], that the horizontal size of the considered atmospheric region is equal to the length of the latitudinal circle at latitude of 50° N, which is $L_h \approx 27{,}000$ km. On the horizontal boundaries of this circle of latitude, we use periodic boundary conditions (see [7]). The simulation was carried out using a wave source (1) with AGW amplitude $W_0 = 0.1$ mm/s. The used range of horizontal phase velocities $c_h \sim 50$ - 200 m/s corresponds to AGWs with relatively large vertical wavelengths that can propagate from the Earth's surface to the upper layers of the atmosphere. The number of wavelengths along the circle of latitude is $n = 32$. This corresponds to the horizontal wavelength $\lambda_h = L_h/n \approx 840$ km and AGW periods $\tau = \lambda_h/c_h \sim 4.7 - 1.2$ h for the range of c_h values indicated above. The step between the nodes of the horizontal grid of the numerical model is $\Delta x = \lambda_h/16$, and the computational time step was automatically chosen to be $\Delta t \approx 2.9$ s. The vertical grid of the model covers altitudes from the earth's surface up to 600 km and contains 1024 unequally spaced nodes. The vertical grid spacing varies from 12 m near the ground to 3 km near the upper boundary, so about 70% of the grid nodes are located in the lower and middle atmosphere.

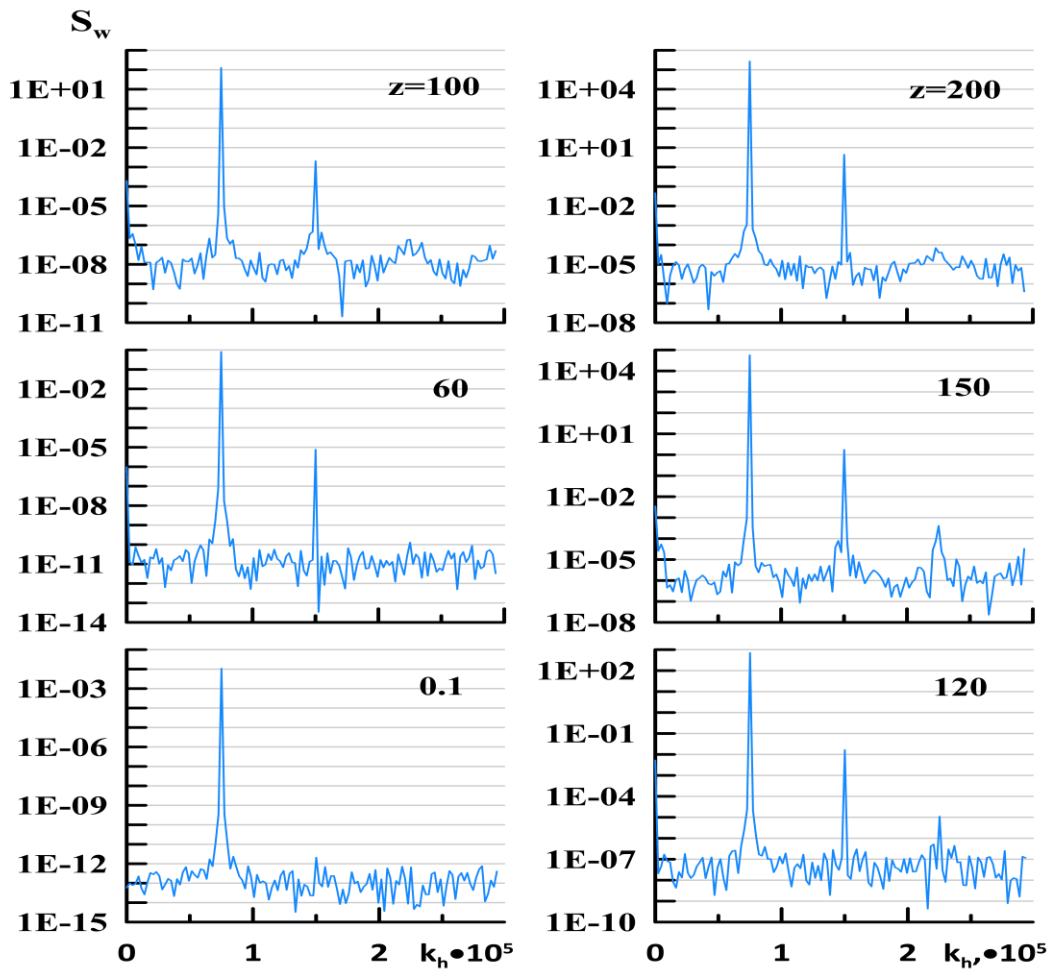

Figure 1. Spectral density, S_w, of model variations of the vertical velocity (in m^3/s^2) depending on k_h (in m^{-1}) on horizontal planes located at different heights (indicated by numbers in km) at the model time $t = 10$ h after the turning on the wave source (1) on the Earth's surface with $W_0 = 0.1$ mm/s and horizontal phase velocity $c_h = 50$ m/s.

The spatial spectra of the simulated hydrodynamic fields in terms of the horizontal wave number are calculated for horizontal planes located at fixed heights and moments of the model time. On such a plane, the values of the simulated hydrodynamic variables are approximated by the sum of the cosine and sine Fourier transforms using the least-squares method. Such calculations are equivalent to the Lomb-Scargle method of spectral analysis [21, 22]. Fig. 1 shows the vertical velocity spectra at different heights in the middle and upper atmosphere at the model time t = 10 h after the wave source (1) was switched on. It can be seen that a peak with $k_h = k_{h1} = 2\pi/\lambda_h$ dominates near the wave source at a height of 0.1 km. At heights of the mesosphere and thermosphere in the spectra in Fig. 1, additionally to the main peak of the primary AGW with $k_h = k_{h1}$, there are peaks at multiple wavenumbers $k_{h2} = 2k_{h1}$ and $k_{h3} = 3k_{h1}$. These peaks correspond to secondary wave modes that arise due to the nonlinearity of the hydrodynamic equations.

Figures 2 and 3 are similar to Fig. 1, but for later times, respectively, t = 20 h and t = 40 h after turning on the wave source. One by one consideration of Figs. 1 – 3 shows that the amplitude of the peak corresponding to the primary AGW increases as the wave energy propagates to high altitudes after turning on the wave source on the earth's surface. Correspondingly, the spectral peaks of secondary AGWs increase also.

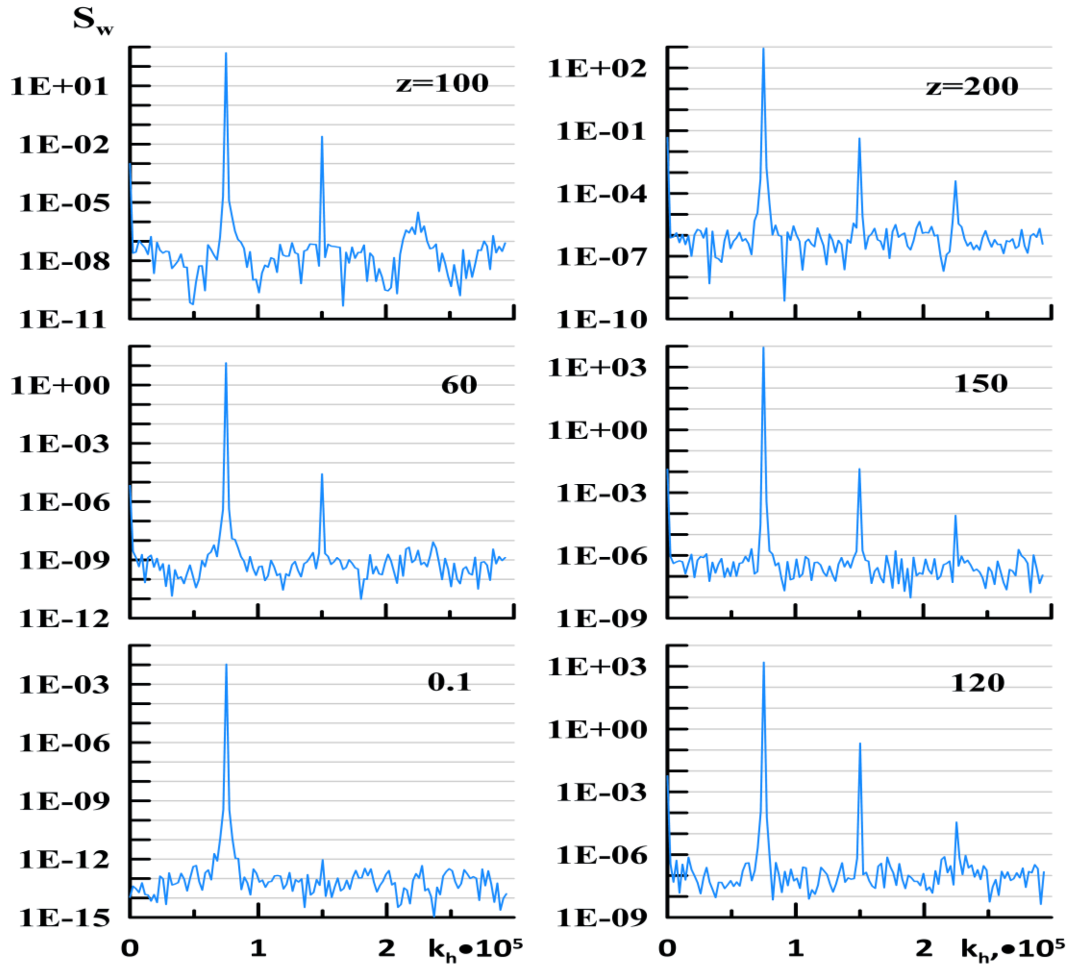

Figure 2. Same as Fig. 1, but for t = 20 h.

In particular, the peaks of the third harmonic with $k_h = 3k_{h1}$ are relatively small in Figs. 1 and increase in Fig. 2 and Fig. 3. This shows the gradual development of the spectrum of secondary AGWs as a result of continuous nonlinear interactions during the propagation of atmospheric AGWs from the Earth's surface to the heights of the thermosphere.

In this paper, the AtmoSym high-resolution nonlinear model is used to simulate the spectrum of primary waves generated by wave sources at the lower boundary of the model and the spectrum of secondary modes generated by these primary waves at different heights of the middle and upper atmosphere. Examples are given showing the gradual formation of the spectrum of secondary waves after the inclusion of a wave source in the model. It is shown that a short time after the source of plane waves is turned on at the lower boundary of the model, the spectrum consists of a peak corresponding to the primary AGW. Later, peaks of secondary wave modes appear in the spectra with horizontal wave numbers that are multiples of the wave numbers of the primary AGW.

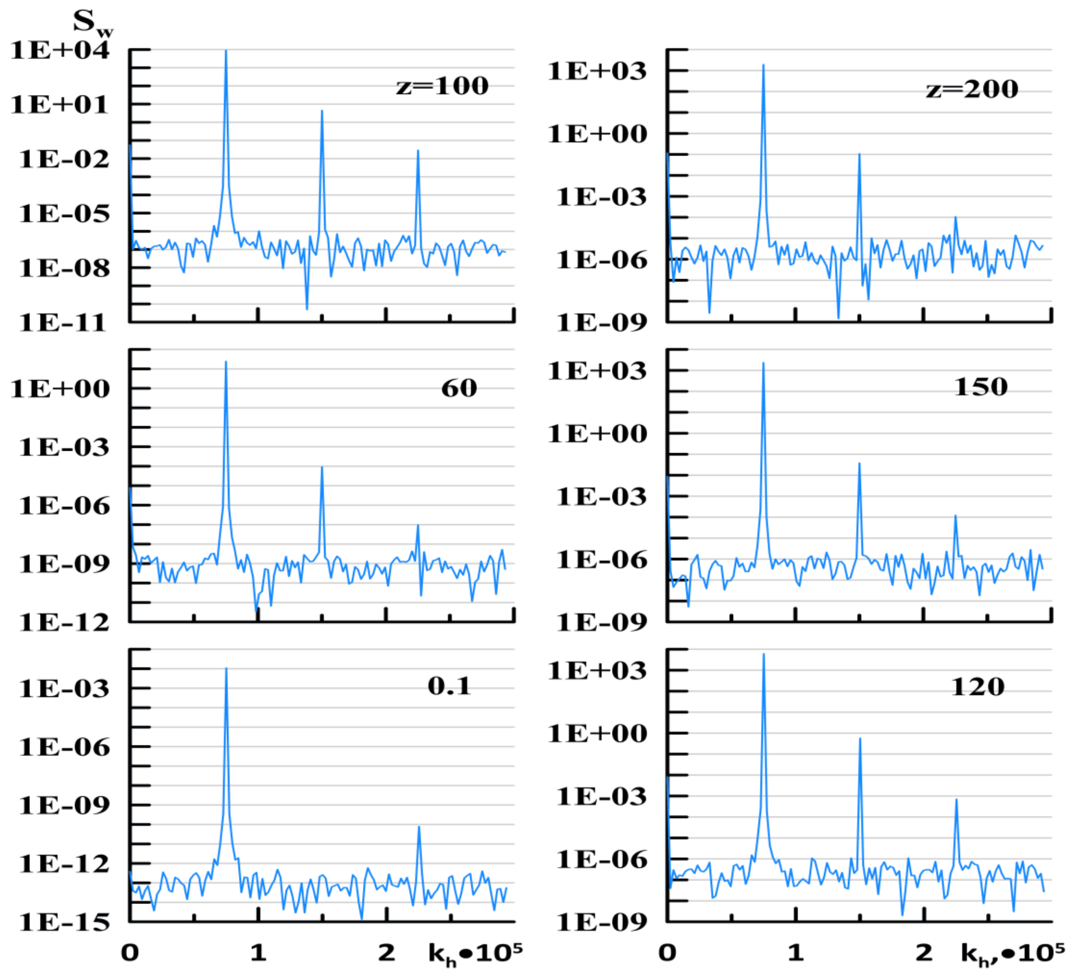

Figure 3. Same as Fig. 1, but for *t* = 20 h.

4. CONCLUSION.

In this work, limited computational power allowed to carry out simulation only with relatively large horizontal grid steps and analyze only the primary wave and the first two spectral peaks of the secondary modes. In the future, similar simulations with smaller steps are required in order to study the features of the formation of the spectrum of secondary AGWs in a wider range of wave numbers.

This study was financially supported by the Russian Science Foundation (grant 22-27-00171).

REFERENCES

[1] Yiğit, E., Medvedev, A.S., Aylward, A.D., Hartogh, M., Harris, J., "Modeling the effects of gravity wave momentum deposition on the general circulation above the turbopause", Journal of Geophysical Research Atmospheres, 114, D07101, https://doi.org/10.1029/2008JD011132 (2009).

[2] Miyoshi, Y., Fujiwara, H., Jin, H., Shinagawa, H., "A global view of gravity waves in the thermosphere simulated by a general circulation model", Journal Geophysical Research Space Physics, 2014, 119, 5807– 5820, https://doi.org/10.1002/2014JA019848 (2014).
[3] Fritts, D.C., Wang, L., Werne, J., "Gravity wave–fine structure interactions: A reservoir of small-scale and large-scale turbulence energy", Geophysical Research Letters, 36(19), L19805, https://doi.org/10.1029/2009GL039501 (2009).
[4] Fritts, D.C., Wan, K., Werne, J., Lund, T., Hecht., J.H., "Modeling the implications of Kelvin-Helmholtz instability dynamics for airglow observations", Journal of Geophysical Research Atmospheres, 119, 8858–8871, https://doi.org/10.1002/2014JD021737 (2014).
[5] Yu, Y., Hickey, M.P., Liu, Y., "A numerical model characterising internal gravity wave propagation into the upper atmosphere", Advances in Space Research, 44, 836–846, https://doi.org/10.1016/j.asr.2009.05.014 (2009).
[6] Liu, X., Xu, J., Liu, H.-L., Ma, R. "Nonlinear interactions between gravity waves with different wavelengths and diurnal tide", Journal of Geophysical Research Atmospheres, 1139(8), D08112, https://doi.org/10.1029/2007JD009136 (2008).
[7] Gavrilov, N.M., Kshevetskii, S.P., "Numerical modeling of the propagation of nonlinear acoustic-gravity waves in the middle and upper atmosphere", Izvestiya Atmospheric Oceanic Physics, 50(1), 66–72, https://doi.org/10.1134/S0001433813050046 (2014)
[8] Vadas, S.L., Fritts, D.C., "The importance of spatial variability in the generation of secondary gravity waves from local body forces", Geophysical Research Letters, 29(20), 1984, https://doi.org/10.1029/2002GL015574 (2002).
[9] Fritts, D.C., Vadas, S.L., Wan, K., Werne, J. A. "Mean and variable forcing of the middle atmosphere by gravity waves", Journal of Atmospheric and Solar-Terrestrial Physics, 68(3-5), 247 – 265, https://doi.org/10.1016/j.jastp.2005.04.010 (2006).
[10] Smith, R.B., Nugent, A.D., Kruse, C.G., David C. Fritts, D.C., Doyle, J.D., Eckermann, S.D., Taylor, M.J., Dörnbrack, A., Uddstrom, M., Cooper, W., Romashkin, P., Jensen, J., Beaton, S., "Stratospheric gravity wave fluxes and scales during DEEPWAVE", Journal of Atmospheric Sciences, 73, 2581 – 2869, https://doi.org/10.1175/JAS-D-15-0324.1 (2016).
[11] Bacmeister, J.T., Schoeberl, M.R., "Breakdown of vertically propagating two-dimensional gravity waves forced by orography", Journal of Atmospheric Sciences, 46, 2109–2134, (1989).
[12] Franke, P.M., Robinson, W.A., "Nonlinear behavior in the propagation of atmospheric gravity waves", Journal of Atmospheric Sciences, 56, 3010–3027, (1999).
[13] AtmoSym, 2017, "A multiscale model of the atmosphere from the Earth's surface up to 500 km", http://atmos.kantiana.ru/language/en/ (last visit 15.02.2023).
[14] Kikoin, I.K., "Tables of physical quantities", Atomizdat Press, Moscow, 272-279, (1976).
[15] Townsend, A.A., "Excitation of internal waves by a turbulent boundary layer", Journal of Fluid Mechanics, 22, 241-252, (1965).
[16] Townsend, A.A., "Internal waves produced by a convective layer", Journal of Fluid Mechanics, 24, 307-319, (1966).
[17]. Picone, J.M., Hedin, A.E., Drob, D.P., Aikin, A.C., "NRLMSISE-00 empirical model of the atmosphere: Statistical comparisons and scientific issues", Journal of Geophysical Research Atmospheres, 107, 1468, https://doi.org/10.1029/2002JA009430 (2002).
[18]. Gossard, E.E., Hooke, W.H., "Waves in the Atmosphere: Atmospheric Infrasound and Gravity Waves: Their Generation and Propagation". Elsevier Sci. Publ. Co. 1975. 456 p.
[19]. Gavrilov, N.M., Kshevetskii, S.P., Koval, A.V., "Verifications of the high-resolution numerical model and polarization relations of atmospheric acoustic-gravity waves", Geoscientific Model Development, 8, 1831–1838, https://doi.org/10.5194/gmd-8-1831-2015 (2015).
[20]. Gavrilov, N.M., Kshevetskii, S.P., Koval, A.V., "Decay times of atmospheric acoustic–gravity waves after deactivation of wave forcing", Atmospheric Chemistry and. Physics, 22, 3713-3724, https://doi.org/10.5194/acp-22-13713-2022 (2022).
[21]. Lomb, N., "Least-squares frequency analysis of unequally spaced data", Astrophysics and Space Science, 39(2), 447–462, (1976).
[22]. Scargle, J.D., "Statistical aspects of spectral analysis of unevenly spaced data", Astrophysical Journal Part 1., 263, 835-853, (1082).